Power optimisation of a heaving buoy in a wave-enhancing contraction (+)

Onno Bokhove, P. Grieve, J. Kim, J. Lee, O. Naar, H. Thompson,
Exeter 13-06-2025
£: CDT2 Fluid Dynamics, teaching

Leeds Institute for Fluid Dynamics, UK

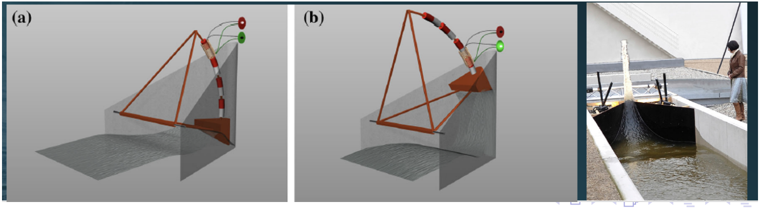

Outline

Overview of our work on the dynamics of:

- a novel wave-energy device, B. et al (2019, 2020, IEEE2024).
- Based on extreme and extremely-high water waves, [e.g., Kadomtsev & Petviashvilli 1970, Benney & Luke 1964, Luke 1967, Kodama (2010, 2018), B. and Kalogirou 2016, Choi et al. (2022, 2024)].
- Inspired by the 2010 bore-soliton-splash:

https://www.youtube.com/watch?v=YSXsXNX4zW0

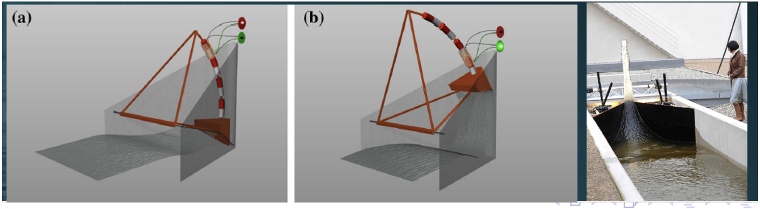

Outline

Our variational, mathematical and numerical, (non)linear wave-to-wire model consists of three coupled components:

- (i) hydrodynamics, using nonlinear potential flow with (free) water surface,
- (ii) buoy motion in 1D, using (vertical) position and velocity, with magnets leading to
- (iii) power generation, using charge and current equations via coil(s), and a load.

I will present: variational principle (full) model, partial model results, including first generator measurements, and open alleys.

Model partitioning

It is ideally placed in a breakwater or in an array of contractions moored at sea. Model partitioning:

- (iii) generator model with prescribed magnet motion,
- (ii)–(iii) a buoy-generator sub-model, and
- (i)–ii) a hydrodynamic wave and buoy sub-model.

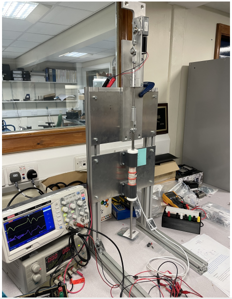

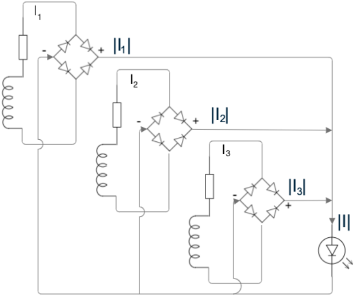

Novel wave-energy device in a breakwater contraction

Proof of principle: `https://www.youtube.com/watch?v=SZhe_SOxBWo&t=254s`.
Sketch wave amplification in contraction with angle θ_c:

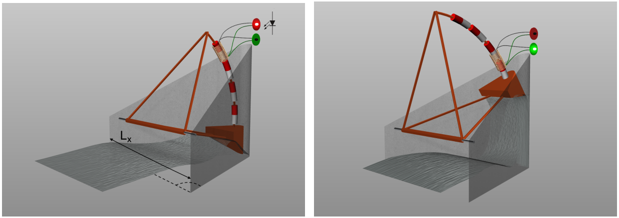

Grand variational principle of novel wave-energy device

Equations of motion follow from variational principle (blue=waves, red=buoy, green=EM-generator, coupling):

$$
\begin{aligned}
0 =& \delta \int_0^T \rho \int_0^{L_x} \int_{R(t)}^{l_y(x)} \int_0^h -(\partial_t \phi + \frac{1}{2}|\nabla \phi|^2)\mathrm{d}z - gh(\frac{1}{2}h - H_0) \\
& \underline{- \frac{1}{2\gamma}\Big(F_+(\gamma(h - h_b(Z,x)) - \lambda)^2 - \lambda^2\Big)}\mathrm{d}y\mathrm{d}x \\
& MW\dot{Z} - \frac{1}{2}MW^2 - MgZ + (L_i I - \underline{K(Z)})\dot{Q} - \frac{1}{2}L_i I^2 \mathrm{d}t
\end{aligned}
$$

velocity $\mathrm{u} = \nabla\phi(x,y,z,t)$, depth $h(x,y,t)$, rest depth H_0, buoy $h_b(Z,x) = Z - K - \tan\theta(L_y - x)$, piston $R(t)$, coupling function $\gamma_m G(Z) = K'(Z)$, buoy mass M, keel height K, buoy coordinate $Z(t)$, buoy velocity $W(t) = \dot{Z}$, charge $Q(t)$, current $I(t) = \dot{Q}$.

Mathematical modelling water-buoy: PDEs

- Potential-flow water-wave dynamics (Laplace equation in interior, kinematic & Bernoulli equations at free surface):

$$\begin{aligned}
\delta\phi: &\quad \nabla^2\phi = 0 \quad \text{in} \quad \Omega\\
(\delta\phi)|_{z=h}: &\quad \partial_t h + \nabla\phi\cdot\nabla h = \phi_z \quad \text{at} \quad z = h\\
\delta h: &\quad \partial_t\phi + \frac{1}{2}|\nabla\phi|^2 + g(z - H_0) - \lambda = 0 \quad \text{at} \quad z = h.
\end{aligned}$$

- Coupled elliptic Laplace equation to hyperbolic free-surface equations; (Lagrange) **multiplier** λ (neg. pressure on buoy).

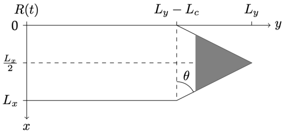

(b) Top view of the tank and buoy, outlining the tank's dimensions and how the buoy fits the shape of the contraction.

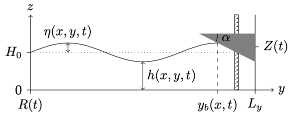

(c) Side view at time t, with the buoy constrained to move vertically.

Mathematical modelling buoy-surface: inequality constraint

- Define $F_+(q) \equiv \max(q, 0)$.
- Karush-Kuhn-Tucker inequality conditions satisfied at every space-time x, t-position are:

$$\delta\lambda : \lambda = -[\gamma(h - h_b) - \lambda]_+ = -F_+(\gamma(h - h_b) - \lambda)$$
$$\Longrightarrow \underline{h(x,t) - h_b(Z,x) \le 0}, \lambda \le 0, \lambda(h - h_b) = 0.$$

- For csts $\gamma, b > 0$ (-), approximations of F_+ include:

$$F_+(q) = \frac{1}{2}q + \sqrt{b^2 + \frac{1}{4}q^2} \rightarrow_{b\to 0} \max(q, 0) \quad \text{with}$$
$$F_+'(q) = \frac{1}{2} + \frac{\frac{1}{4}q}{\sqrt{b^2 + \frac{1}{4}q^2}} \rightarrow_{b\to 0} \Theta(q).$$

Mathematical modelling buoy-generator: ODEs

- Solve 3D Maxwell's eqns for cylindrical magnet-single-coil set-up: reduction from PDEs to 4 ODEs with coupling function $G(Z) = K'(Z)$.
- Add resistance R_i, R_c & (Shockley) load $V_s(I)$ to submodel:

$$\begin{aligned}
\delta W: \quad \dot{Z} =& W,\\
\delta Z: \quad M\dot{W} =& -Mg\underline{-\gamma_m G(Z) I} - \int_0^{L_x}\int_0^{l_y(x)} \lambda \,\mathrm{d}y\mathrm{d}x\\
\delta I: \quad \dot{Q} =& I,\\
\delta Q; \quad L_I \dot{I} =& \underline{\gamma_m G(Z)\dot{Z}} - (R_i + R_c) I - V_S(I).
\end{aligned}$$

Mathematical model generator: multiple coils

Multiple coils $i, j = 1, \dots, N_i$ after ideal rectification s.t. $I_i \to |I_i|$ connected in parallel:

- Current equations with mutual induction M_{ij}:

$$L_I^{(i)} \dot{I}_i + M_{ij} \dot{I}_j = \sum_{i=1}^{N_q} \gamma_m G_i(Z) \dot{Z} - V_S^{(i)}(I_j).$$

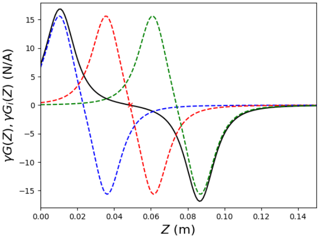

Mathematical modelling buoy-generator: loads

- Shockley load represting parallel-connected LEDs:

$$V_S^{(i)}(I_j) = \frac{n_q V_T I_i}{|I_i|} \ln\left(1 + \sum_{k=1}^{N_i} \frac{|I_k|}{I_{sat}}\right)$$

- Butler-Volmer battery model for small β:

$$V_s^{(i)}(I_j) \approx \frac{I_i}{|I_i|} \frac{\operatorname{asinh}(|I|/I_s)}{q_v/2 + \beta q_v \frac{|I|/I_s}{\sqrt{1+(|I|/I_s)^2}}}$$

- Laboratory test set-up: resistor R after rectification $|I|$ connected in parallel

$$V_S^{(i)}(I_j) = R\frac{I_i}{|I_i|}|I| = R\frac{I_i}{|I_i|}\sum_{j=1}^{N_i}|I_j|.$$

Optimisation wave-energy device: geometry

Surrogate linear modelling geometry angle/rest depth θ_c-H_0:

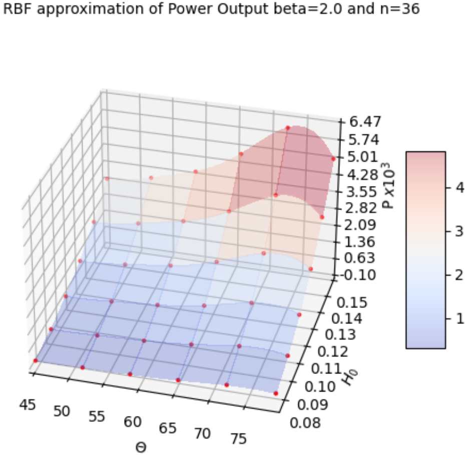

Optimisation wave-energy device: coils

Compare power 1-coil vs. simple 3-coil-in-parallel, lin.:

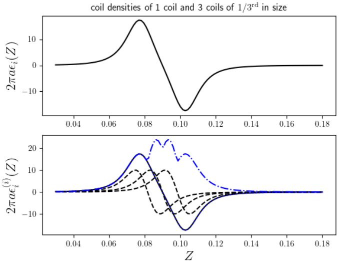

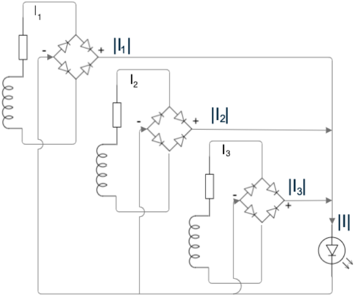

Optimisation wave-energy device: coils

1-coil vs. simple 3-coil-in-parallel power P_g, lin. (B. et al. 2024):

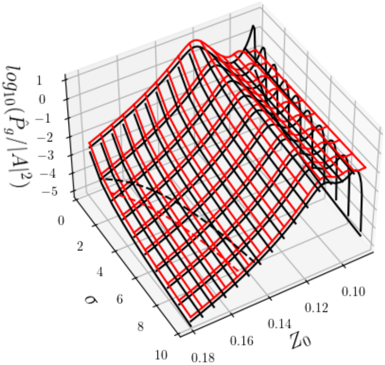

Optimisation wave-energy device: multiple coils

Open query: convergence (implicit mid-point/Brown) time intregators with absolute signs and multiple integrating factors.

- Two-coil model, two cases $I_1, I_2 > 0, < 0$ and $I_1 < 0, > 0; I_2 > 0, < 0$:

$$
\begin{aligned}
L\dot{I}_1 + M\dot{I}_2 =& G_1(Z)\dot{Z} - \mathrm{sign}(I_1)R(|I_1| + |I_2|)\\
M\dot{I}_1 + L\dot{I}_2 =& G_2(Z)\dot{Z} - \mathrm{sign}(I_2)R(|I_1| + |I_2|)
\end{aligned}
$$

- Interim transformation with sign-factor $s_2 = \mathrm{sign}(I_1)\mathrm{sign}(I_2)$:

$$
\begin{pmatrix} I_1 \\ I_2 \end{pmatrix} = \frac{1}{2}(I_{10} + s_2 I_{20}) \begin{pmatrix} 1 \\ s_2 \end{pmatrix} e^{\frac{-2R(t-t_j)}{(L+s_2 M)}} + \frac{1}{2}(I_{10} - s_2 I_{20}) \begin{pmatrix} 1 \\ -s_2 \end{pmatrix}
$$

$$
\frac{\mathrm{d}(I_{10} + s_2 I_{20})}{\mathrm{d}t} = \frac{(G_1(Z) + G_2(Z))\dot{Z}}{L + s_2 M} e^{\frac{2R(t-t_j)}{(L+s_2 M)}} \equiv f_1(t)
$$

$$
\frac{\mathrm{d}(I_{10} - s_2 I_{20})}{\mathrm{d}t} = \frac{(G_1(Z) - s_2 G_2(Z))\dot{Z}}{L - s_2 M} \equiv f_2(t).
$$

Laboratory and model results generator

In summary:

- One-coil measurements and ideal-rectifier model agree reasonably well. Observed peak/mean values: $(1.884, 0.921)\mathrm{V}$; predicted ones: $(1.843, 0.736)\mathrm{V}$.
- Ideal rectified-in-parallel and three-phase rectified genrator perform best.
- Three-coil model overpredicts by factor three and including mutual-coil induction further increases overpredictions. Observed peak and mean values: $(2.341, 1.122)\mathrm{V}$; predicted ones $\approx (7.203, 2.504)\mathrm{V}$. Parameter values: $1/T_{period} = 2.6\mathrm{Hz}$, $R = 100\mathrm{Ohm}$, $l_2 = 0.035\mathrm{m}$.

Analysis (numerical) of inequality constraints

Strategy on buoy-water surface coupling (work in progress):

- Goal is to solve Bernoulli & KKT inequality equations:

$$\delta h: \quad \partial_t \phi + \frac{1}{2}|\nabla \phi|^2 + g(z - H_0) - \lambda = 0 \quad \text{at} \quad z = h.$$
$$\delta \lambda : \lambda = -[\gamma(h - h_b) - \lambda]_+ = -F_+(\gamma(h - h_b) - \lambda)$$
$$\Longrightarrow \underline{h(x,t) - h_b(Z,x) \leq 0}, \lambda \leq 0, \lambda(h - h_b) = 0.$$

- Analyse rest-flow case, when $\phi = 0$ with $h_b(Z,x) = Z - K - \tan\theta(L_y - x)$.
- Analyse "simpler" problem of a ball with position $Z(t)$ falling under gravity to a flat surface such that $Z(t) \geq 0$. **Done.**
- Use Firedrake's in-built inequality-constraint solvers.

VP with Benny-Luke water waves

VP-model of Benney-Luke water waves (cf. Eq. (32) in B. & Kalogirou 2016) coupled to buoy (2D-gradients):

$$\begin{aligned}0 =&\delta\int_0^T\int_0^{L_x}\int_{R(t)}^{l_y(x)} -h\partial_t\phi-\frac{1}{2}\mu\nabla h\cdot\partial_t(\nabla\phi)\\&-\frac{1}{2}|\nabla\phi|^2)-gh(\frac{1}{2}h-H_0)\\&-\mu(\nabla q\cdot\nabla\phi-\frac{3}{4}q^2)-\frac{1}{2\gamma}\Big(F_+(\gamma(h-h_b)-\lambda)^2-\lambda^2\Big)\mathrm{d}y\mathrm{d}x\\&-MZ\dot{W}-\frac{1}{2}MW^2-MgZ\mathrm{d}t.\end{aligned}\tag{1}$$

Midpoint/Brown time integrators

- Convergent solver for modified midpoint (MMP) time discretisation of model with CG-FEM has not been found.
- We therefore consider Brown's midpoint scheme (MMP') with $\{h, Z, \lambda, q\}$ at mid-time $t^{n+1/2}$ & $\{\phi, W\}$ at entire times t^n:

$$
\begin{aligned}
0 =&\delta \sum_{n=0}^{N_t} \int_0^{L_x} \int_{R(t)}^{l_y(x)} -h^{n+1/2}\frac{(\phi^{n+1}-\phi^n)}{\Delta t} - \frac{1}{2}\mu\nabla h^{n+1/2}\cdot\frac{(\nabla\phi^{n+1}-\nabla\phi^n)}{\Delta t}\\
&-\frac{1}{2}h^{n+1/2}|\frac{1}{2}\nabla(\phi^{n+1}+\phi^n)|^2) - gh^{n+1/2}(\frac{1}{2}h^{n+1/2}-H_0) - \mu(\frac{1}{2}\nabla q^{n+1/2}\cdot\nabla(\phi^{n+1}+\phi^n)\\
&-\frac{3}{4}(q^{n+1/2})^2) - \frac{1}{2\gamma}\Big(F_+(\gamma(h^{n+1/2}-h_b(Z^{n+1/2}))-\lambda^{n+1/2})^2-(\lambda^{n+1/2})^2\Big)\mathrm{d}y\mathrm{d}x\\
&-MZ^{n+1/2}\frac{(W^{n+1}-W^n)}{\Delta t} - \frac{1}{2}M(\frac{1}{2}(W^{n+1}+W^n))^2 - MgZ^{n+1/2}\mathrm{d}t,
\end{aligned} \tag{2}
$$

with variations $\{h^{m+1/2}, Z^{m+1/2}, \lambda^{m+1/2}, q^{m+1/2}, \phi^m, W^m\}$.

Rest flow

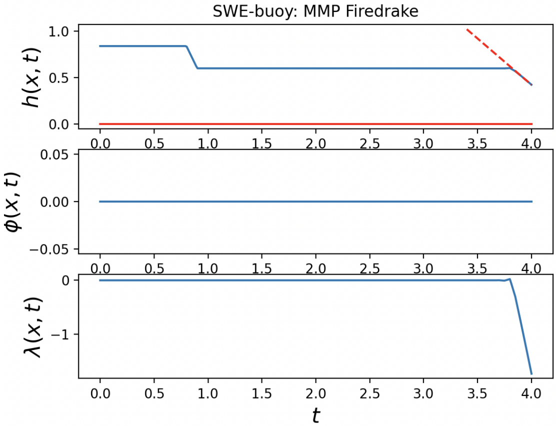
SWE-buoy: MMP Firedrake
$h(x,t)$
1.0
0.5
0.0
$\phi(x,t)$
0.05
0.00
−0.05
$\lambda(x,t)$
0
−1
0.0 0.5 1.0 1.5 2.0 2.5 3.0 3.5 4.0
t

Rest flow

To date, only rest flow works with MMP' & some dynamics with MMP, noting that:

- "Soft" inequality approach with MMP cannot guarantee constraint on h^{n+1} due to extrapolation with constraining at half $n+1/2$ time.
- Brown's MPP' can by construction guarantee constraint.
- Explicit schemes cannot work, unless $\{h^{n+1/2}, \phi^{n+1}, Z^{n+1/2}, \lambda^{n+1/2}\}$ are intrinsically coupled, see also work by Bueler, Bueler & Farrell in Firedrake (hard-inequality solvers).
- Open alley: relationship between softening parameter $b, \Delta t$ and preconditioners.

Soft inequality: bouncing ball and billiards' tests

Bouncing ball results with MMP and MMP', phase plots:

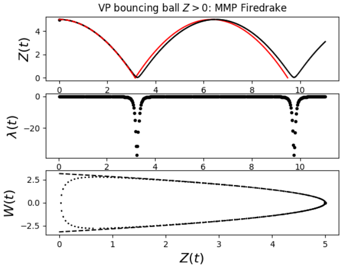

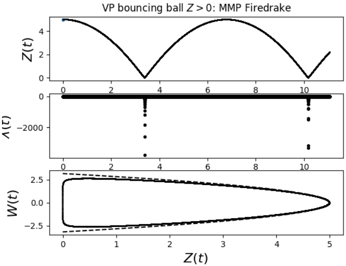

Novel wave-energy device: concluding remarks

- **Brief overview given** of wave-energy device, based on extreme-wave amplification in a contraction. Achieved (linear) modelling with VPs & geometric numerical integrators.
- Rest-flow case as stepping stone works.
- For dissipative terms in the electro-magnetic generator, either integrating factors required: or smoothing of signs. Agreement or factor three off experiments. Multiple coils in parallel give more yield.
- Achieved first geometric and coil optimizations.

Novel wave-energy device: future work

- Future work: inequality constraints, optimisation, real-time control using Pontryagin's principle, surrogate modelling & ML.
- A laboratory set-up of the wave-energy device is in progress, in steps:
  a)hanging dry, driven generator, and
  b) full hydrodynamic coupling in our $2\mathrm{m}$ wave tank.
- New wave-energy idea: test flexible electronic sheet to generate energy & as surf-zone damping (Dr Jeamin Lee).

https://www.sciencedirect.com/science/article/abs/pii/S1364032121007590

Thanks very much for your attention ...

- B., Kalogirou, Zweers 2019: From bore-soliton-splash to a new wave-to-wire wave-energy model. *Water Waves* **1** 10.1007/s42286-019-00022-9
  Bore-soliton-splash: https://www.youtube.com/watch?v=YSXsXNX4zW0&list=FL6mc7mUa6M4Bo2VkD970urw
- B., A. Kalogirou, D. Henry, G. Thomas 2020: A novel rogue-wave-energy device with wave amplification and induction actuator. *Int. Marine Energy J.* **30**.
- Choi, Kalogirou, Lu, B., Kelmanson 2024: A study of extreme water waves using a hierarchy of models based on potential-flow theory. *Water Waves* https://doi.org/10.1007/s42286-024-00084-4
- B., Bolton, H. Thompson, Geometric power optimisation of a rogue-wave energy device in a (breakwater) contraction. 8th IEEE Conference on Control Technology & Applications (CCTA) (2024) 6 pp. Preprint https://eartharxiv.org/repository/view/7260/

Aspects of wave-energy device: results to date

To date the following modelling and results have been obtained:

- Full nonlinear wave-to-wire model formulated for both equality and inequality constraints of the 2D buoy-free-surface water interface (B et al 2019).
- Full numerical 2D linearised (shallow-water) model of wave-to-wire model with equality constraint (B. et al 2019, Bolton et al. 2021, B et al IEEE2024).
- *Optimisations* done for the contraction geometry using full and (Latin-hypercube) surrogate modelling (B et al IEEE2024).

Aspects of wave-energy device: results to date

. . . following modelling and results have been obtained:

- Full nonlinear 3D potential-flow water-wave submodel & numerical simulations (Gidel et al 2022, Choi et al 2022/2024, Lu et al 2024), implementing model's space-time variational principle (VP). 2^{nd} order in time, higher-order in space.
- Full nonlinear buoy-generator submodel & numerics based on time-discrete VP plus symmetric/consistent dissipative terms.
- Optimisation (linear) buoy-generator submodel by analysing 1-coil and 3-coils-in-parallel generators. Partially succesful comparison measurements of generator.

Why variational principles (VPs)? Advantages:

- When (main) dynamics has a VP, multiple coupled equations are succintly described by one space-time VP.
- Associated with a VP are conservation properties of associated PDEs/ODEs.
- Within the *(finite-element) environment Firedrake*, the time-discrete VP can be implemented directly, with automated generation of (complicated 3D+1D) weak forms of the equations. Adjoint solvers, optimal control.
- Advantages: enormous reduction in development time, efficient, flexible, higher-order spectrally-accurate space discretisations plus (automatic) preservation of discrete forms of conservation properties.